Grandis and Menvielle *Earth, Planets and Space* (2015) 67:121
DOI 10.1186/s40623-015-0290-3

Earth, Planets and Space
a SpringerOpen Journal

FULL PAPER Open Access

Thin-sheet electromagnetic modeling of magnetovariational data for a regional-scale study

Hendra Grandis[1*] and Michel Menvielle[2]

Abstract

Naturally existing electromagnetic (EM) fields recorded at the surface of the Earth can be used to infer the electrical conductivity distribution of the subsurface. In the magnetovariational sounding (MVS) technique, the transient variations of orthogonal components of the Earth's magnetic field are measured. In the frequency domain, the magnetic transfer function relates the vertical component to the horizontal components of the magnetic field. This paper describes the thin-sheet modeling of MVS data on a regional scale. The integrated conductivity variations in the thin-sheet model were estimated by applying the Markov chain Monte Carlo (MCMC) inversion algorithm. The application of this method to MVS data from the Finland part of the Fennoscandian Shield has illustrated the utility of both the thin-sheet approximation and MCMC inversion modeling. The conductivity anomalies obtained from this study confirmed the regional-scale geology of the area.

Keywords: Geomagnetic deep sounding; Markov chain Monte Carlo; Inverse modeling

Background

Transient variations of the Earth's main magnetic field due to solar wind activity serve as the primary field in electromagnetic (EM) induction methods, which allow for the estimation of the subsurface electrical conductivity distribution. The magnetovariational sounding (MVS) technique is a specific EM method where only orthogonal components of the Earth's magnetic field variations (H_x, H_y, H_z) are measured. In the frequency domain, the relationship between the vertical component and the orthogonal horizontal components of the magnetic field reflect the conductivity of the medium. In the EM community, the MVS technique is also known as the geomagnetic deep sounding (GDS) method. The data generated from this method are the magnetic transfer functions, presented as magnetic induction vectors or induction arrows (Lilley and Arora 1982; Hobbs 1992). Important studies using this method are mainly at the crustal scale, due to the deep investigation depths and lateral integrating effect of the magnetometer array recordings at long periods or low frequencies (e.g., Heinson and Lilley 1993; Armadillo et al. 2001; Gurk and Schnegg 2001). With the availability of three-dimensional (3D) EM modeling, MVS data can also be interpreted as the 3D resistivity distribution of the subsurface (e.g., Kanda and Ogawa 2014; Wang et al. 2014).

This paper describes the application of thin-sheet modeling of MVS data from a regional-scale EM study of Finland. We consider that the so-called thin-sheet approximation is appropriate for modeling MVS data due to the relatively limited frequency band of MVS data in general. In this study, 3D subsurface conductivity variations were assumed to be confined to a thin layer. Hence, the model parameters were the integrated conductivities over the thickness of the thin layer. This simplification is appropriate for modeling MVS data, which are mostly sensitive to lateral variations of conductivity (Robertson 1988; Wang and Lilley 1999; Handa 2005).

We first briefly review the concept of thin-sheet EM modeling and the Markov chain Monte Carlo (MCMC) algorithm for inversion. The MCMC inversion technique has previously been applied for geo-electromagnetic data in relatively simple 1D models with satisfactory results, for example, magnetotelluric (MT; Grandis et al. 1999; Guo et al. 2011), DC resistivity (Schott et al. 1999; Maiti et al.

* Correspondence: grandis@geoph.itb.ac.id
[1]Institut Teknologi Bandung, Jalan Ganesha 10, Bandung 40132, Indonesia
Full list of author information is available at the end of the article

Springer

© 2015 Grandis and Menvielle. This is an Open Access article distributed under the terms of the Creative Commons Attribution License (http://creativecommons.org/licenses/by/4.0), which permits unrestricted use, distribution, and reproduction in any medium, provided the original work is properly credited.

2011), and Controlled-Source Audio-frequency MT (CSAMT; Grandis and Sumintadiredja 2013) studies. Despite the simplicity of the 1D models in geoelectromagnetics, their inversions involve highly non-linear problems demanding non-linear or global search approaches to avoid fundamental limitations of the linearized approach (Sen and Stoffa 1996; Sambridge and Mosegaard 2002). With similar homogeneous model parameterization involving only the physical property, while the geometry is held fixed, the extension of the MCMC algorithm to thin-sheet inversion modeling was deemed straightforward. The application of the MCMC technique to invert both synthetic and field data with thin-sheet models has led to encouraging results (Grandis et al. 2002; 2013). We present the modeling of MVS data from the Finland part of the Fennoscandian Shield and discuss the results.

Methods

In EM geophysics, the thin-sheet model is commonly used to represent 3D conductivity variations with a limited vertical extent. Such an approximation is generally valid in large-scale studies when the heterogeneities are confined to a layer with a thickness significantly smaller than the penetration depth of EM fields. This quasi-3D model consists of a thin layer with variable conductance (i.e., integrated conductivity over the thickness of the thin layer). Thin-sheet modeling significantly simplifies the solution of Maxwell's equations describing EM fields in a quasi-3D medium. Generally, the integral equation method is used to resolve the governing equations (e.g., Vasseur and Weidelt 1977; McKirdy et al. 1985; Schmucker 1995). The computation domain covers only the anomalous zone, where the conductance differs from that of the normal host medium, represented by either a homogeneous or stratified environment (Fig. 1).

In EM geophysics, numerous algorithms employ the integral equation method for thin-sheet modeling. In addition to those already cited, Fainberg et al. (1993) extended the formulation for the thin sheet at the surface in order to apply it at depth using either a natural or artificial primary field. Lechman et al. (2011) compared thin-sheet and 3D models, while Sun and Egbert (2012) extended the use of thin-sheet models for global EM induction problems. EM thin-sheet modeling by Vasseur and Weidelt (1977) was integrated with our existing MCMC inversion algorithm. In particular, we used the modified algorithm where the thin sheet is located at depth (Terra and Tarits 1991; Terra 1993).

The thin sheet containing heterogeneities was discretized into uniform rectangular blocks, for each of which the conductance was assumed to be constant. In the frequency domain, the system of linear equations for the total electric field of all blocks located in the heterogeneous layer involves the Green kernel matrix associated with the electric field at a given block due to a unitary dipole in another block. We used the Gauss-Seidell method (Press et al. 1997) to solve the system of linear equations in order to obtain the electric fields (E_x, E_y), from which the orthogonal magnetic fields (H_x, H_y, H_z) were calculated. In the MT method, the transfer function relating electric and magnetic fields is the complex impedance tensor, while in the MVS or GDS technique we are interested in the relationship between the orthogonal components of the magnetic field. In the frequency domain, the vertical component is related to the horizontal components of the magnetic field by the single station magnetic transfer functions $A(\mathbf{r},\omega)$ and $B(\mathbf{r},\omega)$:

$$H_z(\mathbf{r},\omega) = A(\mathbf{r},\omega)\,H_x(\mathbf{r},\omega) + B(\mathbf{r},\omega)\,H_y(\mathbf{r},\omega), \quad (1)$$

where $\mathbf{r}$ and ω are position and angular frequency, respectively. Magnetic transfer functions are complex, with real and imaginary parts, and are often represented as magnetic induction vectors and plotted as arrows on maps. The length (L) and direction (θ) of the real part induction arrow are obtained from:

$$L_R(\mathbf{r},\omega) = \sqrt{\left(\mathrm{Re}(A(\mathbf{r},\omega))\right)^2 + \left(\mathrm{Re}(B(\mathbf{r},\omega))\right)^2} \quad (2a)$$

$$\theta_R(\mathbf{r},\omega) = \tan^{-1}\left(\frac{\mathrm{Re}(B(\mathbf{r},\omega))}{\mathrm{Re}(A(\mathbf{r},\omega))}\right) \quad (2b)$$

Similar equations also hold for the imaginary part of the induction arrows. Note that the direction angle in Eq. 2b is clockwise from North since in geomagnetism, the x- and y-axes are directed to the north and east, respectively. The direction of the real part of the induction

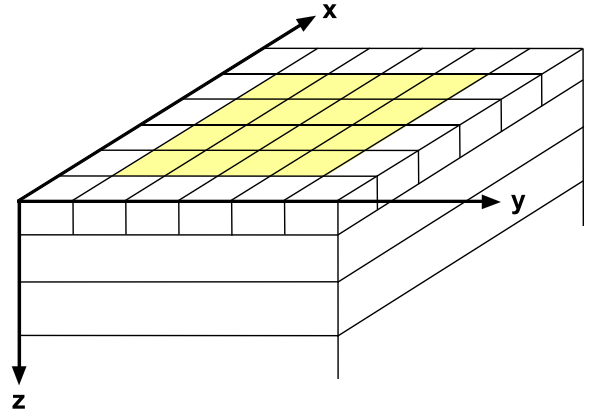

Fig. 1 Heterogeneous thin-sheet model at the surface, with normal (*white*) and anomalous (*yellow*) conductance embedded in a layered (1D) host medium. The resistivities and thicknesses of the 1D host medium are held fixed and determined from *a priori* information

arrows is inverted in accordance with Parkinson's convention, such that they point towards more conductive zones (Lilley and Arora 1982; Hobbs 1992).

The inversion modeling consisted of determining the conductance of blocks in the thin sheet (Fig. 1). In the Bayesian inference context, the solution of an inverse problem can be expressed by the posterior distribution of the model parameters that combine the likelihood function and the prior distributions of the model parameters. Markov chain Monte Carlo (MCMC) is a sampling technique that allows the estimation of the posterior probability distribution (Sen and Stoffa 1996; 2013). We adopted the MCMC technique with the Gibbs sampler to generate the chains. Therefore, the transition probability governing the Markov chain is available in explicit form and is represented by the probability of a conductance value for a given block, based on the current conductance configuration of the other blocks. For a limited number of possible conductance values for each thin-sheet block, the conditional probability can be calculated directly (Grandis 1994).

We assumed that the parameters for the 1D host medium were fixed and known. For each thin-sheet block, the discrete values of possible conductance with a homogeneous probability were available as *a priori* information. These values covered a sufficiently large interval, from low to high conductance, to minimize bias in the inverse problem solution. Starting from a homogeneous thin sheet, the conductance of each block was sequentially updated in turn. A sequence of models (or states) were developed that adhered to the fundamental Markov chain rule (i.e., the probability of the next model depends only on the current model). The transition probability of the Markov chain governed the sequence of models in the chain, which were a subset of the finite number of possible models. Without further details, we assumed that the ergodicity of the chain held. This property guaranteed the convergence of the Markov chain to the simulated posterior distribution. After sufficient iterations, the Markov chain was independent of the initial model and exhibited a stationary state described by its invariant probability. In this case, the invariant probability of the constructed Markov chain was the posterior probability of the model parameters (i.e., the inverse problem solution; Heerman 1990; Robert 1996).

The MCMC inversion algorithm was tested to invert the synthetic MT impedance tensors and the magnetic induction vectors associated with thin-sheet models, with satisfactory results (Grandis et al. 2002). Both resistive and conductive anomalies were relatively equally well resolved due to the addition of the Gauss-Seidell iterations in the misfit evaluation. Grandis et al. (2002) underlined the importance of properly discretizing the *a priori* conductance interval into possible conductance values for the thin-sheet blocks. The MCMC algorithm was also applied to invert real GDS data from an area spanning the eastern margin of the Bohemian Massif to the West Carpathians in Europe. The conductance map obtained from this study correlates well with the regional geology (Grandis et al. 2013) and allows for a more quantitative analysis of the conductivity anomalies present in the area.

Inversion of MVS data

The MVS dataset used in this study was taken from the Finland sector of a regional-scale EM study of the Fennoscandian Shield. Several field measurement campaigns were conducted, in part by the Department of Physics, University of Oulu, Finland, from which the data were obtained by the UFR Physique de la Terre et des Planètes, Université Paris Sud, France (Menvielle, pers. comm.). The available data were magnetic transfer functions at 143 stations for periods of 100, 300, and 1000 s. However, only data for periods of 300 and 1000 s were used in the inversion in order to conform to the validity of the thin-sheet approximation. The observation stations were randomly scattered over Finland. Details of the data processing and preliminary analyses can be found in Pajunpaa (1987), Korja and Hjelt (1993), and others. The study area represents one of the oldest parts of the Earth's crust, the Baltic Shield. Therefore, there remains significant interest in analyzing existing data from this region. The EM study data were further complemented with data from many other field campaigns involving MVS, MT, and also airborne EM measurements that covered the whole of the Fennoscandian Shield (Engels et al. 2002; Korja 2007).

The data for all periods exhibited similar characteristics. Figure 2 shows the MVS data presented as the real part of the induction arrows for the period of 300 s. The coastline shown in Fig. 2 serves as an approximate reference only and is of low resolution, such that some data plotted offshore. The direction of the real induction arrows point towards more conductive zones. In Fig. 2, there are coherences and consistencies in the direction of the real induction arrows over a relatively large area, especially at the eastern and central parts of the study area. We also observed abrupt changes in the direction over very limited or narrow areas, which may be associated with very conductive anomalies (e.g., at the northern part of Bothnian Bay and in the south-eastern part of the study area). However, from visual observations alone, it is difficult to qualitatively delineate conductivity anomalies based solely on the induction arrow map.

For the inversion, the induction vector most representative of each 50 by 50 km block was selected. We evaluated the difference of each vector with its neighbors in the same block using a least-squares approach. Hence, we

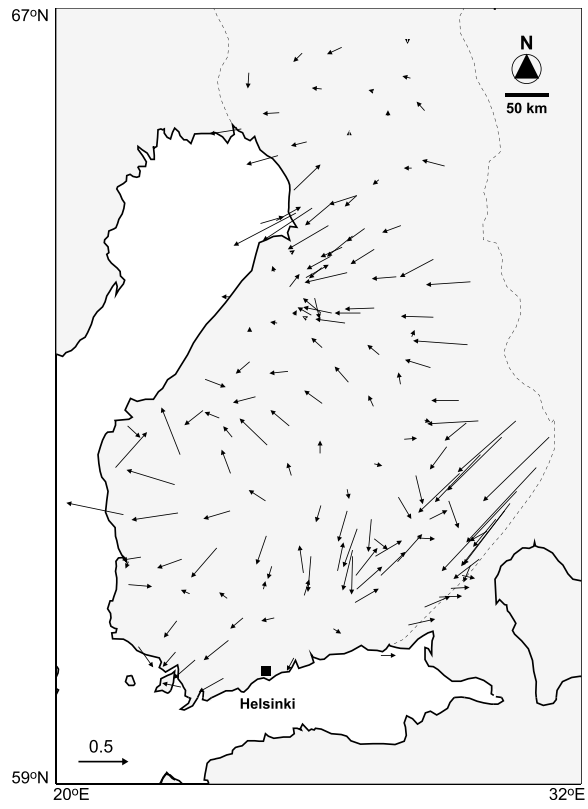

Fig. 2 Field data from magnetovariational sounding (MVS) over Finland, presented as real induction arrows at a period of 300 s. Data were inverted in accordance with Parkinson's convention; therefore, the real induction arrows point towards more conductive zones. Geographical coordinates of map boundaries (using the Mercator projection) and the position of Helsinki are given for reference

obtained the most coherent induction vector for each of the blocks in the thin sheet. In this way, spurious effects caused by the interpolation of the MVS data into a more regular grid were avoided. As a consequence, some blocks had no data at all, and these were less constrained in the inversion process. In addition, there were some instances of data outside of the land area (offshore), since the data were placed at the center of the constructed blocks.

From previous studies synthesized by Jouanne (1991) and Roussignol et al. (1993), we established a stratified (1D) medium to host the heterogeneous thin layer at a depth representing conductivity variation in the study area. The 1D model was composed of five layers:

- from 0- to 10-km depth, where resistivity was 1000 Ohm
- from 10- to 30-km depth, where resistivity was 10 Ohm
- from 30- to 40-km depth, where resistivity was 100 Ohm
- from 40- to 140-km depth, where resistivity was 1000 Ohm
- greater than 140-km depth, where resistivity was 10 Ohm

The thin sheet at 10–30-km depth (i.e., the second layer) was initially discretized into 12 by 18 blocks, each 50 by 50 km in dimension. This choice was dictated by the validity of the thin-sheet approximation and also by the computational resources available. In terms of EM induction, a layer may be regarded as a thin sheet if the electric field is virtually unchanged in magnitude and phase across the depth of the layer. More particularly, conditions for the thin-sheet approximation are as follows: (a) the sheet thickness must be negligibly small compared with the skin depth of the material directly beneath it; (b) the sheet thickness must be small compared with the skin depth of the material within the sheet; and (c) the grid spacing must be small compared with the skin depth of the material directly beneath the sheet (Weaver 1994). The available 300-s MVS data used in this modeling did not strictly meet all three conditions. The skin depth of the 300-s variation in the 100-Ohm underlying layer was ~87 km. As the 20-km thickness of the thin sheet was significantly less than this skin depth, condition (a) was met. The 50-km dimension of the grid spacing was only a little smaller than this skin depth, so condition (c) was marginal. In the 10-Ohm thin-sheet layer, the skin depth was ~27 km, which was comparable to the 20-km thickness of the thin sheet, so condition (b) was not met. However, while the 300-s data do not strictly meet all of the conditions set out by Weaver (1994), we consider that overall the thin-sheet approximation still holds since we are more interested in large-scale variations.

We used *a priori* conductance values from 4 to 10,000 Ohm^{-1} (or Siemens/m), which were quasi-logarithmically discretized to represent resistive to conductive anomalies in the region. For a thin sheet with 20-km thickness, those *a priori* conductance values corresponded to resistivity values of 5000 down to 2 Ohm. Starting with normal conductance in the thin sheet (i.e., 2000 Ohm^{-1}), the inversion was performed for up to 20 iterations. The posterior model was obtained by averaging the conductance values of each block from the last 15 iterations and the results are presented in Fig. 3. Significant spatial variations of conductance were obtained from the average model. The discretization of the thin sheet did not allow for more regular conductance variations from block to block. Using this approach, applying an additional constraint equivalent to the smoothness constraint of 1D inversions (e.g., Grandis et al. 1999) is difficult and would require discretizing the thin sheet into a larger number blocks, with most not constrained by observation. In contrast, the thin-sheet approximation imposed a minimum block size compared to the thickness of the thin layer, such that the approximation still held.

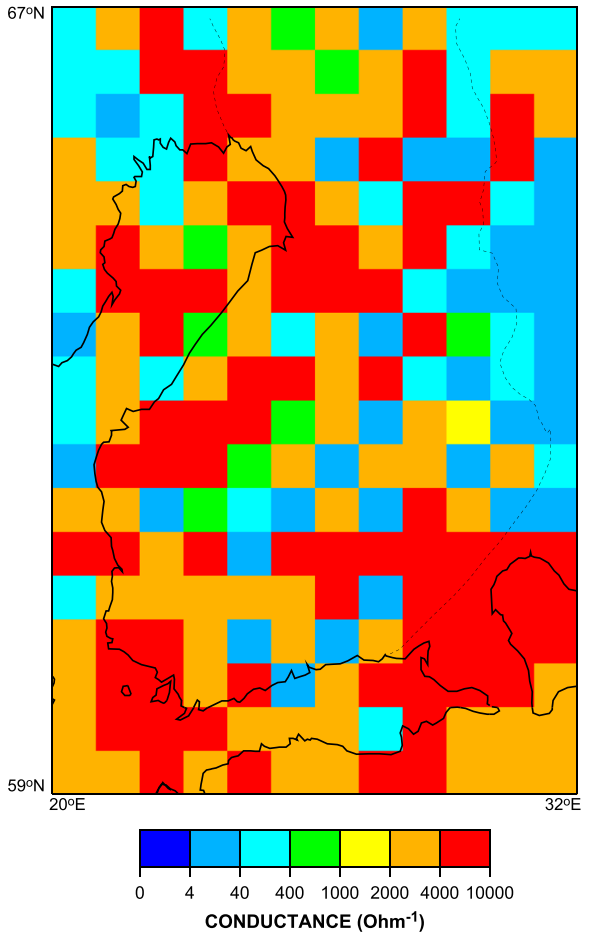

Fig. 3 Conductance variation within the thin-sheet model at 10–30-km depth, as obtained from the inversion of magnetovariational sounding (MVS) data with the initial block size (i.e., 50 by 50 km)

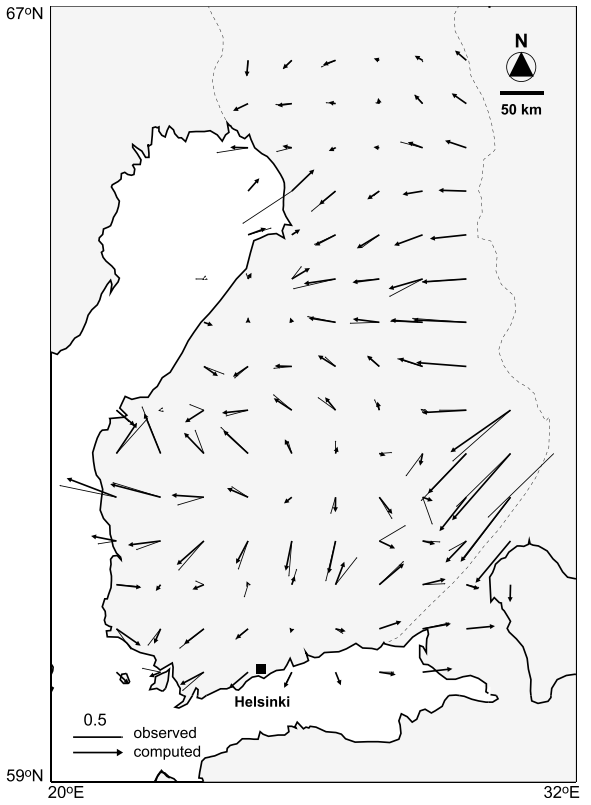

Fig. 4 Selected field data (*thin line*) representing the observed data at the center of each block in the thin sheet and the calculated response of the inverse model (*thick arrows*), both for the period of 300 s

Despite significant spatial variations in conductance within the average model, the calculated response of the inverse model was broadly in agreement with the observed data (see Fig. 4 for real induction arrows at 300 s). Except for one block situated to the North of Bothnian Bay, where observed and calculated induction arrows were in opposite directions, the magnitude and direction of the induction arrows were within the 20 % error floor used in the inversion. Such a relatively large error floor was chosen to roughly represent the estimated data accuracy, which was not available, and to provide a sort of relaxation in the inversion. The calculated data at several blocks were too small, such that they appear only as arrowheads, and in other cases, only observed data are visible in Fig. 4. Note also that for one of the easternmost blocks, no calculated data were plotted.

Further analysis and post-processing steps were considered necessary in order to propose a more meaningful interpretation of the posterior model. We thus resampled the thin-sheet conductance map, obtained from the initial inversion, into 25×25 km blocks and used a simple 5×5 block 2D moving average filter to obtain a new interpolated conductance map. Figure 5 shows the more interpretable model, which showed significant correlation with the geological and tectonic setting of the study area.

Results and discussion

In general, our results showed that the upper and middle crust between 10- and 30-km depth in the Fennoscandian Shield is very heterogeneous. The crustal conductivity variations expressed by the initial conductance map covered a large range, from 4 to 10,000 Ohm^{-1}. The smoothing of the posterior model reduced the conductance interval to a relatively limited range (i.e., from 400 to 4000 Ohm^{-1}). Such a smoothing process also introduced a smearing effect, such that long and narrow anomalies appear broader in the final conductance map. However, we still observed distinct geological or tectonic units based on their conductance.

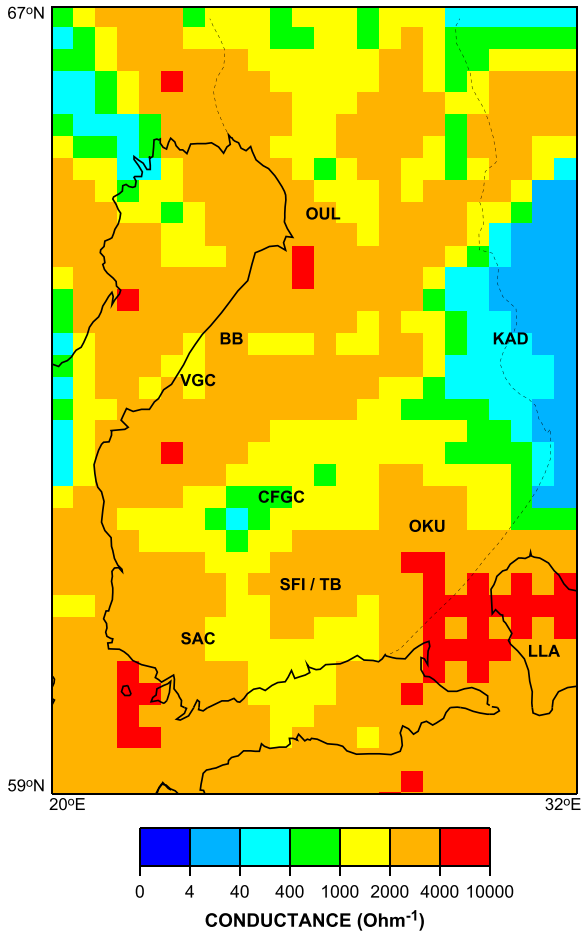

Fig. 5 Conductance map from the inversion of magnetovariational sounding (MVS) data after the rediscretization of blocks to 25 by 25 km. The interpreted conductivity anomalies are the: Central Finland Granitoid Complex (CFGC), Southern Finland conductivity anomaly (SFI),Tampere Belt (TB), Bothnian Belt (BB), Vaasa Dome or Vaasa Granitoid Complex (VGC), Oulu (OUL), Outokumpu (OKU), and Lake Ladoga (LLA) anomalies, and the Karelian Domain (KAD)

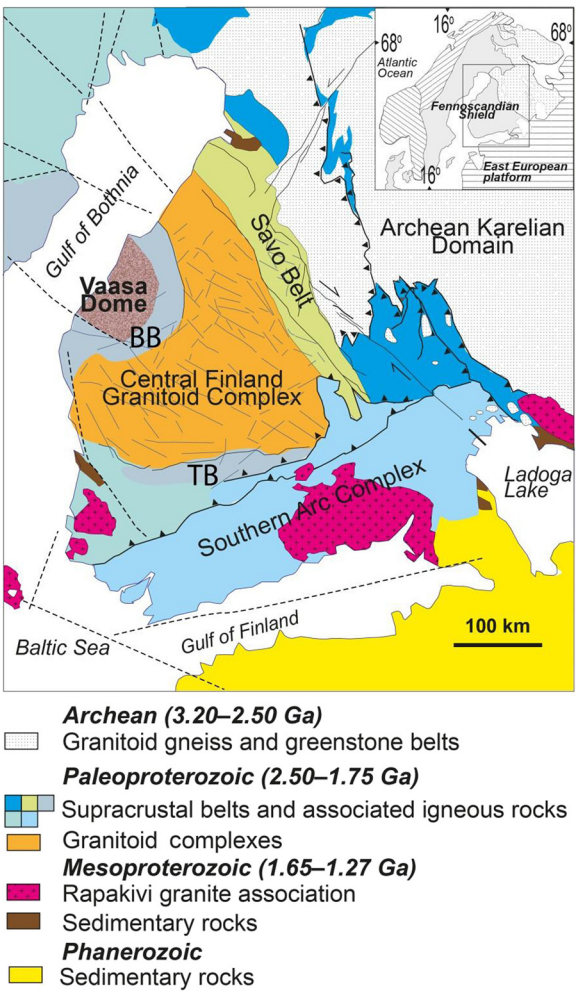

Fig. 6 Tectonic map of the Fennoscandian Shield used for the interpretation of conductivity anomalies observed in the inversion results (after Korja et al. 2009)

Two main conductive features were present, except for a restricted resistive zone in the eastern part of Finland, and can be further interpreted from the final conductance map (Fig. 5). The results showed highly conductive zones (2000–4000 Ohm^{-1}), which form narrow and elongated belts that delineate moderately conductive and more homogeneous blocks (1000–2000 Ohm^{-1}). These dominant features can be correlated with the regional geology and tectonics shown in Fig. 6 (Korja et al. 2002; Korja et al. 2009; Chopin et al. 2012).

The results showed that the central part of Finland is dominated by relatively moderate conductive zones (1000–2000 Ohm^{-1}) with a spatially limited and isolated block reaching as low as 400 Ohm^{-1}. Although continental crust was generally represented by a less conductive (more resistive) medium, a unit with moderate conductance correlated well with the Central Finland Granitoid Complex (CFGC). As pointed out by Korja et al. (2002), most of the upper crust (0–30 km) was characterized by good conductors (higher than 1000 Ohm^{-1}).

The results also showed that large conductive zones (2000–4000 Ohm^{-1}) surround much of the CFGC in the central part of Finland, with a restricted resistive zone in the east. As part of these large conductive zones, the relatively narrow and elongated region that borders the CFGC to the south is the Southern Finland conductivity anomaly (SFI), which is partially associated with the Tampere Belt (TB). Further to the south is the Southern Finland sedimentary-volcanic complex, also known as the Southern Finland Arc Complex (SAC). Our results showed that the latter is less homogeneous and can be further differentiated into at least three sub-blocks (i.e., conductive–less conductive–conductive, from west to east). The less conductive part coincided with the area

in which the Rapakivi granite association unit is found (Fig. 6).

In the northwest, facing the Gulf of Bothnia, the conductive anomaly referred to as the Bothnian Belt (BB) surrounds the less conductive Vaasa Dome or Vaasa Granitoid Complex (VGC). We can infer that the conductive anomaly of the Bothnian Belt continues further to the northwest (i.e., to the Gulf of Bothnia), although the blocks in this area were not directly constrained by the data. The conductive anomalies surrounding the CFGC also extend to the north, as the Oulu anomaly (OUL), and to the southeast, as the Outokumpu (OKU) and Lake Ladoga (LLA) anomalies. The latter was characterized by very conductive anomalies at irregular spots (greater than 4000 Ohm^{-1}), which are likely artifacts resulting from the averaging process (see Fig. 5).

Although not constrained by the data, the resistive area (between 4 and 400 Ohm^{-1}) on the eastern border of Finland can be associated with granitoid-gneiss complexes known as the Karelian Domain (KAD). This resistive zone, along with the other conductive zones discussed above, is in good agreement with results obtained for the same depth by Korja et al. (2002) and Engels et al. (2002) using multi-sheet models. In much of the literature discussing EM modeling results from the study area (e.g., Hyndman et al. 1993; Korja and Hjelt 1993) the elongated conductive anomalies are associated with graphite- and sulfide-bearing rocks, geologically identified as schist belts.

Conclusions

We have presented thin-sheet modeling of MVS data using the MCMC inversion algorithm. In thin-sheet modeling, lateral variations in the subsurface conductivity structure are expressed as integrated conductivity over the thickness of the sheet (i.e., conductance), such that vertical conductivity variations within each layer are unknown. This type of approximation is in agreement with the physics of EM induction, which is more sensitive to the conductivity-thickness product than to conductivity variation with depth. However, by assuming the thickness of the thin sheet is fixed, we obtained a model with only lateral conductivity variation.

The necessity to comply with the thin-sheet approximation and limitations of the MCMC method led us to use blocks with relatively large horizontal dimensions. The use of smaller blocks to achieve a better lateral resolution may have led to difficulties in the intensive exploration of a high-dimensional model space, as necessitated in the MCMC inversion method (e.g., Rosas-Carbajal et al. 2014). Magnetometer array studies are usually performed with a large spatial sampling distance (several to tens of kilometers); hence, the lateral resolution of the MVS data is limited. However, information from subsurface large-scale conductivity structures is useful in understanding the development of the crustal-scale tectonics of a study area.

We applied thin-sheet modeling with the MCMC inversion algorithm to MVS data from the Finland part of the Fennoscandian Shield and generated satisfactory results. The main features of the conductivity structures from our study correlate well with the regional geology and tectonics of the area. The obtained conductance map also confirms the results of previous studies by Pajunpaa (1987), Korja and Hjelt (1993), Engels et al. (2002), and Korja et al. (2002), among others. The crustal conductivity structure in the Fennoscandian Shield appears to be very heterogeneous, reflecting the complex geological and tectonic processes of the past. Readers are referred to the results of the BEAR Working Group, synthesized in Engels et al. (2002) and Korja et al. (2002), for more detailed tectono-geological implications of the conductivity structures obtained from various similar models. However, the evolution of the Fennoscandian Shield is beyond the scope of our study.

Competing interests

The authors declare that they have no competing interests.

Authors' contributions

HG was responsible for the inversion and for the preliminary draft of the manuscript. MM supervised the interpretation of the results and revised the first draft of the paper up to the submission stage. Both HG and MM involved in revisions up to the final form. Both authors read and approved the final manuscript.

Acknowledgements

The authors are grateful to Toivo Korja and his colleagues at the Department of Physics, Division of Geophysics, University of Oulu, Finland, for providing the processed magnetovariational data used in this study. We also acknowledge the reviewers' careful reading and constructive comments that greatly improved the manuscript.

Author details

[1]Institut Teknologi Bandung, Jalan Ganesha 10, Bandung 40132, Indonesia. [2]Centre d'Etude de l'Environnement Terrestre et Planétaires, 3 Avenue de Neptune, Saint Maur des Fosses F-94107, France.

Received: 15 April 2015 Accepted: 8 July 2015
Published online: 30 July 2015

References

Armadillo E, Bozzo E, Cerv V, De Santis A, Di Mauro D, Gambetta M, Meloni A, Pek J, Speranza F (2001) Geomagnetic depth sounding in the Northern Apennines (Italy). Earth Planets Space 53:385–396

Chopin F, Korja A, Hölttä P (2012) Tectonometamorphic evolution of the Bothian belt within the Svecofennian orogen - a case study for the building of a large dome in the Paleoproterozoic. In: Abstracts of the LITHOSPHERE 2012 Symposium, Espoo—Finland

Engels M, Korja T, BEAR Working Group (2002) Multisheet modelling of the electrical conductivity structure in the Fennoscandian Shield. Earth Planets Space 54:559–573

Fainberg EB, Pankratov OV, Singer BS (1993) Thin sheet modelling of subsurface and deep inhomogeneities. Geophys J Int 113:144–154

Grandis H (1994) Imagerie electromagnetique Bayesienne par la simulation d'une chaine de Markov. Dissertation, Université Paris 7

Grandis H, Sumintadireja P (2013) Quasi-2D resistivity model from inversion of CSAMT (Controlled-Source Audio-frequency Magnetotellurics) data. In:

Abstracts of the HAGI-IAGI Joint Convention, Medan—Indonesia, 28–31 October 2013
Grandis H, Menvielle M, Roussignol M (1999) Bayesian inversion with Markov chains—I. The magnetotelluric one-dimensional case. Geophys J Int 138:757–768
Grandis H, Menvielle M, Roussignol M (2002) Thin-sheet electromagnetic inversion modeling using Monte Carlo Markov Chain (MCMC) algorithm. Earth Planets Space 54:511–521
Grandis H, Menvielle M, Roussignol M (2013) Thin-sheet inversion modeling of geomagnetic deep sounding data using MCMC algorithm. Int J Geophys Article ID 531473 doi:10.1155/2013/531473
Guo R, Dosso SE, Liu J, Dettmer J, Tong X (2011) Non-linearity in Bayesian 1-D magnetotelluric inversion. Geophys J Int 185:663–675
Gurk M, Schnegg PA (2001) Anomalous directional behaviour of the real parts of the induction arrows in the Eastern Alps: tectonic and palaeo-geographic implications. Ann Geofis 44:659–669
Handa S (2005) Electrical conductivity structures estimated by thin sheet inversion, with special attention to the Beppu-Shimabara graben in central Kyushu, Japan. Earth Planets Space 57:605–612
Heerman DW (1990) Computer simulation methods in theoretical physics. Springer-Verlag, Berlin
Heinson GS, Lilley FEM (1993) An application of thin-sheet electromagnetic modelling to the Tasman Sea. Phys Earth Planet In 81:231–251
Hobbs B (1992) Terminology and symbols for use in studies of electromagnetic induction in the Earth. Surv Geophys 13:489–515
Hyndman RD, Vanyan LL, Marquis G, Law LK (1993) The origin of the electrically conductive lower continental crust: Saline water or graphite? Phys Earth Planet In 81:325–344
Jouanne V (1991) Application des techniques statistiques Bayesiennes à l'inversion de données électromagnétiques. Dissertation, Université Paris 7
Kanda W, Ogawa Y (2014) Three-dimensional electromagnetic imaging of fluids and melts beneath the NE Japan arc revisited by using geomagnetic transfer function data. Earth Planets Space 66:39
Korja T (2007) How is the European lithosphere imaged by magnetotellurics? Surv Geophys 28:239–272
Korja T, Hjelt SE (1993) Electromagnetic studies in the Fennoscandian Shield—Electrical conductivity of precambrian crust. Phys Earth Planet In 91:107–138
Korja T, Engels M, Zhamaletdinov AA, Kovtun AA, Palshin NA, Smirnov MY, Tokarev AD, Asming VE, Vanyan LL, Vardaniants IL, BEAR Working Group (2002) Crustal conductivity in Fennoscandia—A compilation of a database on crustal conductance in the Fennoscandian Shield. Earth Planets Space 54:535–558
Korja A, Kosunen P, Heikkinen PJ (2009) A case study of lateral spreading: the Precambrian Svecofennian Orogen In: Ring U, Wernicke B (eds) Extending a Continent: Architecture, Rheology and Heat Budget. Geol Soc Lond Spec Pap 321:225–251
Lechmann SM, May DA, Kaus BJP, Schmalholz SM (2011) Comparing thin-sheet models with 3-D multilayer models for continental collision. Geophys J Int 187:769–783
Lilley FEM, Arora BR (1982) The sign convention for quadrature Parkinson arrows in geomagnetic induction studies. Rev Geophys Space Phys 20:513–518
Maiti S, Gupta G, Erram VC, Tiwari RK (2011) Inversion of Schlumberger resistivity sounding data from the critically dynamic Koyna region using the Hybrid Monte Carlo-based neural network approach. Nonlin Processes Geophys 18:179–192
McKirdy D, McA WJT, Dawson TW (1985) Induction in a thin sheet of variable conductance at the surface of a stratified earth—II: Three-dimensional theory. Geophys J Roy Astr S 80:177–194
Pajunpaa K (1987) Conductivity anomalies in the Baltic Shield in Finland. Geophys J Roy Astr S 91:657–666
Press WH, Flannery BP, Teukolsky SA, Vetterling WT (1997) Numerical recipes: The art of scientific computing, 2nd edn. Cambridge University Press, Cambridge
Robert C (1996) Méthodes de Monte Carlo par Chaînes de Markov. Economica, Paris
Robertson RC (1988) The electromagnetic response of a heterogeneous layer modelled by two thin sheets in a uniformly conducting halfspace. IEEE Trans Geosci Remote Sens 26:2–10
Rosas-Carbajal M, Linde N, Kalscheuer T, Vrugt JA (2014) Two-dimensional probabilistic inversion of plane-wave electromagnetic data: methodology, model constraints and joint inversion with electrical resistivity data. Geophys J Int 196:1508–1524
Roussignol M, Jouanne V, Menvielle M, Tarits P (1993) Bayesian electromagnetic imaging. In: Hardle W, Siman L (eds) Computer Intensive Methods. Physical Verlag, Berlin
Sambridge M, Mosegaard K (2002) Monte Carlo methods in geophysical inverse problems. Rev Geophys 40:1–29
Schmucker U (1995) Electromagnetic induction in thin sheets: integral equations and model studies in two dimensions. Geophys J Int 121:173–190
Schott JJ, Roussignol M, Menvielle M, Nomenjahanary FR (1999) Bayesian inversion with Markov chains—II. The one-dimensional DC multilayer case. Geophys J Int 138:769–783
Sen MK, Stoffa PL (1996) Bayesian inference, Gibbs' sampler and uncertainty estimation in geophysical inversion. Geophys Prospect 44:313–350
Sen MK, Stoffa PL (2013) Global optimization methods in geophysical inversion, 2nd edn. Cambridge University Press, Cambridge
Sun J, Egbert GD (2012) A thin-sheet model for global electromagnetic induction. Geophys J Int 189:343–356
Terra A (1993) Modélisation électromagnétique de deux plaques minces hétérogènes et son application à l'étude de la croûte et du manteau. Dissertation, Université Paris 7
Terra A, Tarits P (1991) Mutual coupling between heterogeneous structures at different depths. In: Abstracts of the 20th IUGG General Assembly, Vienna—Austria, 11–24 August 1991
Vasseur G, Weidelt P (1977) Bimodal electromagnetic induction in non-uniform thin sheets with an application to the northern Pyrenean induction anomaly. Geophys J Roy Astr S 51:669–690
Wang L, Lilley FEM (1999) Inversion of magnetometer array data by thin-sheet modeling. Geophys J Int 137:128–138
Wang L, Hitchman A, Ogawa Y, Siripunvaraporn W, Ichiki M, Fuji-ta K (2014) A 3-D resistivity model of the Australian continent using magnetometer array data. Geophys J Int 198:1171–1186
Weaver JT (1994) Mathematical methods for geo-electromagnetic induction. Research Studies Press Ltd, Taunton, Somerset, England

Submit your manuscript to a SpringerOpen journal and benefit from:

► Convenient online submission
► Rigorous peer review
► Immediate publication on acceptance
► Open access: articles freely available online
► High visibility within the field
► Retaining the copyright to your article

Submit your next manuscript at ► springeropen.com